International Hydrographic Review, LXXVI(1), March 1999

AUGMENTATION OF GPS FOR HYDROGRAPHIC APPLICATIONS UNDER SIGNAL MASKING

by S. RYAN, J. STEPHEN, J.H. KEONG, G. LACHAPELLE [1] and R. HARE [2]

ABSTRACT

In critical coastal water areas where signal masking due to high topographic features is severe, GPS is known to be deficient in either one or both of two characteristics, namely availability and reliability, the latter being associated with the notion of quality assurance. Augmentation of GPS with either GLONASS and/or geostationary satellites, in addition to the use of height and clock constraints is becoming a viable alternative, the more so as cost effective GPS/GLONASS receivers become available. The question as to what degree this combined approach can resolve the above limitations is analyzed herein by first conducting a series of simulations and, second, by validating these simulations with actual marine tests. The simulations use worst-case anisotropic mask angles encountered for specific locations along Canada's Pacific Coast. Availability is evaluated through dilution of precision (DOP), figures of merit, and reliability by internal and external reliability measures. The GPS/GLONASS/geostationary satellites analysis includes simulations with height and clock constraints to determine the impact of these constraints on availability and reliability. Each set of results are compared to GPS to assess the incremental benefits of each type of augmentation. The simulations are validated with actual DGPS/DGLONASS measurements collected on a survey launch off Sidney, B.C., Canada.

[1] Department of Geomatics Engineering.

[2] Canadian Hydrographic Service, Department of Fisheries and Oceans.

INTRODUCTION

The advent of satellite based navigation/positioning systems has dramatically changed hydrographic surveying. In the past, user-owned specialized and expensive positioning systems would be required, however this is being revolutionized by differential GPS (DGPS). The expensive specialized shore-based positioning systems are now being replaced by relatively inexpensive user-owned GPS receivers, supplemented by code based differential GPS corrections. The GPS corrections are available from a variety of sources including free public systems, such as the Canadian Coast Guard's marine radiobeacon DGPS System, and commercial providers who usually charge a user fee.

The horizontal positioning requirements for hydrographic surveying depend on the surveying environment and the equipment used. These requirements are summarized in the following section. In areas such as inlets and fjords where high mask angles occur due to the surrounding mountainous topography, unaided GPS is known to be insufficient to provide the availability and/or accuracy and reliability required. Augmentation of GPS with other systems and/or onboard sensors is the solution to this problem. Two classes of systems can be considered, namely ground - and satellite-based. Ground-based systems include the use of pseudolites that transmits signals similar to GPS. While the use of pseudolites in constricted navigation channels shows promises (MORLEY & LACHAPELLE 1998), their potential use for charting in remote inlets and fjords is more limited due to a variety of operational considerations. In this case, augmentation with other satellite-based systems and on-board sensors constitutes a more cost-effective alternative.

Horizontal Accuracy Requirements

The fourth edition of the International Hydrographic Organization (IHO, 1998) Special Publication No. 44 (S-44) on IHO Standards for Hydrographic Surveys defines minimum positioning accuracy requirements for four orders of hydrographic survey. These orders are summarized in Table 1.

Code based DGPS is a practical and effective method of providing the horizontal positions for hydrographic surveying. Using high performance GPS receivers in normal masking conditions, accuracies of 0.5 - 2.0 m (2DRMS) are attainable. Many hydrographic surveys, however, take place in non-ideal masking conditions. The survey launch must operate close to shore near very high cliffs, which gives rise to extreme anisotropic masking angle conditions. The hydrographic survey requires high availability (low DOP) and highly reliable (free from blunders) positions. The availability and reliability requirements are even greater when the data is to be used for the production of nautical charts. How well does DGPS satisfy the hydrographic surveying availability and reliability requirements under extreme masking conditions? The focus of this paper is to answer this question for DGPS alone and for DGPS augmented with other satellite systems and constraints.

Table 1: Summary of Minimum Standards for Hydrographic Surveys (IHO, 1998)

Order	Special	1	2	3
Examples of Typical Areas	Harbours, berthing areas, and associated critical channels with minimum under-keel clearance	Harbours, harbour approach channels, recommended tracks and some coastal areas with depths up to 100 m	Areas not described in Special Order and Order 1, or areas up to 200 m water depth	Offshore areas not described in Special Order, Orders 1 and 2
Horizontal Accuracy (95% confidence level)	2 m	5 m + 5% of depth	20 m + 5% of depth	150 m + 5 % of depth

The analysis of unaided DGPS and DGPS augmented with other satellite systems and constraints is performed in two parts. Firstly, hydrographic survey line simulations are conducted using unaided DGPS and DGPS augmented with GLONASS and geostationary satellites and two constraints (height and clock). GLONASS is tested in two modes, namely single point and differential (DGLONASS). Geostationary satellites are tested in differential mode. The GLONASS constellation is currently available, however, the use of geostationary satellites to transmit GPS signals is still in the planning stage. The reason to test GLONASS in single point mode is that most public and commercial DGPS services do not have a DGLONASS capability. If geostationary satellites do become available, they will be observable with GPS receivers and the differential mode will therefore be widely available. When the various satellite combinations and constraints are combined, a total of twenty different positions methods were analyzed in simulation mode.

Secondly, a marine test was conducted in Saanich Inlet, B.C. Two integrated GPS/GLONASS Ashtech GG24™ receivers were used for the tests. A clock constraint was implemented using two rubidium frequency standards, while a height constraint was employed using tidal information. In total eight different positioning methods were analyzed for the field test.

For both the simulation and field test the positioning methods were inter-compared, based on the position's availability and reliability. The availability analysis was performed by inter-comparing the horizontal dilution of precision (HDOP). In simulation mode the reliability was analyzed through internal and external reliability measures. The reliability during the field test was measured by analysing the positioning method's ability to detect and remove blunders from the observables. The resulting maximum horizontal position error (HPE) was used as the reliability measure. Before the results from the simulation and the field test are presented, the reliability theory used for the analysis is presented.

RELIABILITY THEORY

Reliability refers to the controlability of observations, that is, the ability to detect blunders and to estimate the effects that undetected blunders may have on a solution [e.g., LEICK, 1995]

Reliability can be sub-divided into internal and external reliability. Internal reliability quantifies the smallest blunder that can be detected through statistical testing of the residuals. This implies that the position solution is not unique, hence redundancy must exist in order to detect a blunder. Once the internal reliability has been determined, external reliability quantifies the impact that an undetected blunder can have on the unknown parameters.

The amount of redundancy (v_i) that each observation adds to the solution is given by

$$v_i = (C_{\hat{f}} C_l^{-1})_{ii}$$

where $C_{\hat{f}}$ is the covariance matrix of the residuals and C_l is the covariance matrix of the observations.

By investigating the following residual covariance matrix, it is evident that individual redundancy numbers for each observation must range from 0 to 1.

$$C_{\hat{f}} = C_l - A\left(A^T C_l^{-1} A\right)^{-1} A^T$$

where A is the design matrix. In order to detect a blunder in an observation, a statistical test must be performed on the residuals. The underlying assumption is that the residuals are normally distributed and that a blunder, while biasing the residual, does not change its variance. There are two types of errors that can be made when performing any statistical test. A Type I error occurs whenever a good observation is rejected. The probability associated with a Type I error is denoted α. A Type II error occurs whenever a bad observation is accepted. The probability associated with a Type II error is denoted β. Figure 1 shows a graphical representation of the relationship between the Type I/II errors and the bias in the standardised residual, called the non centrality parameter δ_o. By selecting values for α and β, δ_o can be determined, as shown in Table 2.

Table 2: Non Centrality Parameter

α	β	δ_o
5.0%	20%	2.80
2.5%	20%	3.10
5.0%	10%	3.24
2.5%	10%	3.52
0.1%	20%	4.12
0.1%	10%	4.57

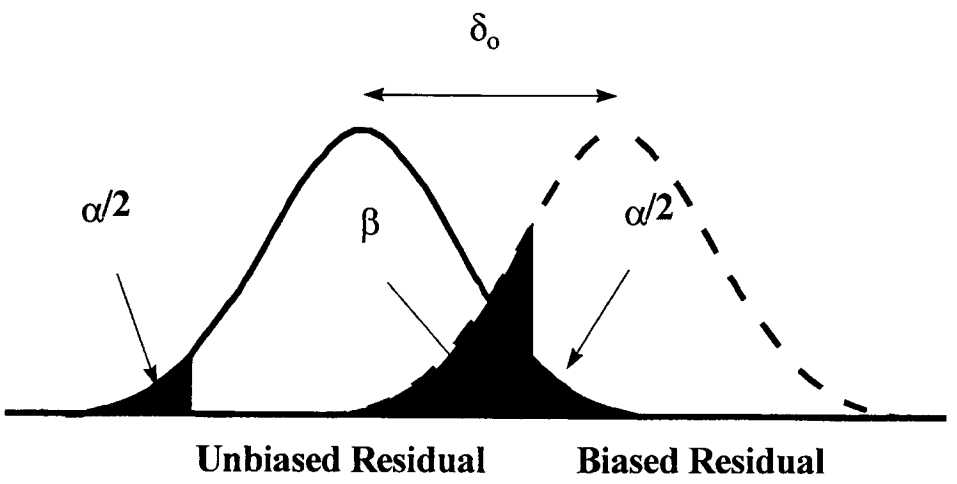

FIG. 1.- Type I/II Errors and Non Centrality Parameter.

Once δ_o is generated, the smallest blunder that can be detected through statistical testing is given by the following equation, and is termed the Marginally Detectable Blunder (MDB).

$$MDB_i \Rightarrow |\nabla_i| = \frac{\delta_o \sigma}{\sqrt{v_i}}$$

Each observation has a different MDB since the redundancy number for each observation is different. Therefore, it is desirable for all of the observations' redundancy numbers to be approximately equal and close to unity, since the position is only as robust as its lowest redundancy number. If this is the case the solution does not have any weaknesses due to blunders.

Once the MDB's for each observation has been calculated, the impact of each blunder on the unknown parameters must be determined. The underlying assumption is that only one blunder can occur at any one time. Therefore, each MDB is applied separately to assess its impact on the parameters as

$$\Delta X_i = -C_x A^T C_l^{-1} \nabla_o$$

where ∇_o is a column vector containing all zero's except for the MDB in the i^{th} position. The above equation reflects the external reliability of the solution. The horizontal error corresponding to each MDB is calculated as

$$\text{Horizontal Error}_i = \sqrt{\Delta\phi_i^2 + \Delta\lambda_i^2}$$

The largest horizontal error is termed the Maximum Horizontal Error (MHE) and represents the external reliability in hydrographic applications.

SIMULATION DESCRIPTION

In order to determine the improvements in availability and reliability obtainable by augmenting DGPS with single point GLONASS (GLO), differential GLONASS (DGLO), differential geostationary satellites (DGEO), and height and clock constraints, two representative survey lines were simulated. The following parameters define the simulation:

a) Satellite Constellations
   1. DGPS
   2. DGPS + GLO
   3. DGPS + DGEO
   4. DGPS + DGLO
   5. DGPS + DGEO + DGLO

b) Constraints
   1. None
   2. Height
   3. Clock
   4. Height + Clock

c) Reliability Parameters:
   1. $\alpha = 0.1\%$, $\beta = 10\%$, and $\delta_0 = 4.57$

d) Other Data:
   1. Date of GPS and GLONASS Ephemerides: July 25, 1997
   2. Duration: 24 hours
   3. Location: Vancouver Island, B.C., Canada, 48° N 123° W
   4. 25 GPS satellites available
   5. 15 GLONASS satellites available
   6. 6 Geostationary satellites available

Since the simulations were being performed for hydrographic applications, high quality receivers were assumed. The clock constraint variance was selected assuming the use of rubidium frequency standards, and the height constraint variance assumed that tidal information was being used. The following observation variances were used for the simulations.

1) DGPS = 1 m^2
2) GLO = 64 m^2
3) DGLO = 1 m^2
4) DGEO = 1 m^2
5) height constraint = 4 m^2
6) clock constraint = 1 m^2

In many cases, one could make the point that a height constraint with a variance lower than 4 m^2 could be used. However, for other cases where the tides are not so well known and other effects such as swell and waves might be significant, the use of a 4 m^2 value is more realistic. In practice, a good quality ovenized quartz clock would also provide good performance, although with a higher variance. A conservative reliability algorithm was used, which assumed that the residual testing was done on an epoch by epoch basis using no a priori knowledge of the trajectory.

The improvements obtained by augmenting DGPS were evaluated by assessing availability and reliability improvements. When the variance of the observations and constraints are the same, the HDOP is based solely on geometry. However in the cases where GLONASS (single point) and/or a height constraint are used to augment DGPS, a weighted HDOP must be calculated, as shown in the following equation:

$$DOP = \sqrt{trace([A^T PA]^{-1})}$$

$$HDOP = \sqrt{NDOP^2 + EDOP^2}$$

$$P = \begin{bmatrix} \frac{\sigma^2_{DGPS}}{\sigma^2_{DGPS}} = 1 & 0 & 0 \\ 0 & \frac{\sigma^2_{DGPS}}{\sigma^2_{GLONASS}} = \frac{1}{64} & 0 \\ 0 & 0 & \frac{\sigma^2_{DGPS}}{\sigma^2_{HEIGHT}} = \frac{1}{4} \end{bmatrix}$$

Since DGPS is the base system, all other variances are referred to it. The weight matrix is unity except when single point GLONASS and/or a height constraint are used. In those cases, the diagonal values for the rows corresponding to the GLONASS satellites (single point) are 1/64, and the height constraint is 1/4, while all of the other entries on the diagonal are unity. In these simulations, the height and clock constraints are added as quasi-observables to the design matrix (A), and therefore are also included in the weight matrix (P).

Although geostationary satellites do not currently transmit GPS signals, several augmentation systems may do so in the future. For the purpose of this simulation, the following six geostationary satellites were simulated, namely

1) INMARSAT-3 @ 180° E
2) INMARSAT-3 @ 64.5° E
3) INMARSAT-3 @ 55.5° W
4) INMARSAT-3 @ 15.5° W
5) Additional SV @ 100° W
6) Additional SV @ 140° W

The elevation angle of a geostationary satellite is a function of the latitude and the relative longitude of the geostationary satellite to the user. Figure 2 shows this relationship for user latitudes varying from 0° to 80° N. A latitude of 48° N was selected for the simulations presented herein, thus the maximum geostationary elevation angle is approximately 32°. This raises an interesting point, namely if a high southern mask angle occur during a survey, geostationary satellites will not have any affect. This will be illustrated in the simulation results section.

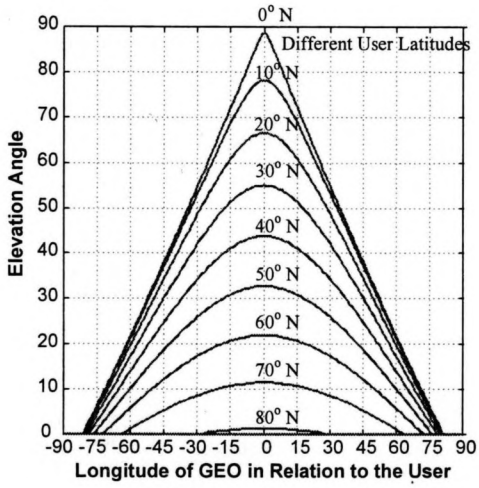

FIG. 2.- Elevation Angle for Geostationary Satellites.

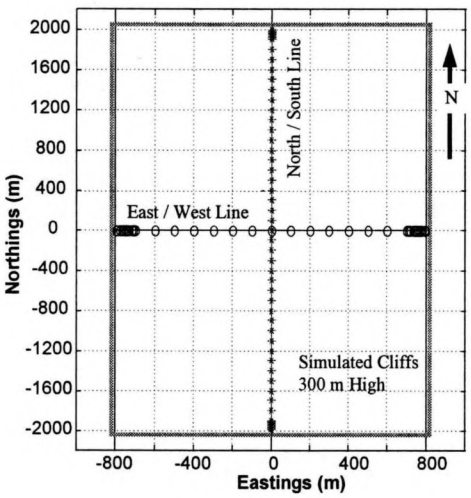

FIG. 3.- Simulated Survey Lines.

Two survey lines were analyzed for a simulated inlet 1600 m by 4000 m with 300 m high cliffs, as shown in Figure 3. Two survey lines were analyzed, namely a East/West and a North/South line, both in the centre of the inlet. Satellite visibility therefore ranged from excellent in the centre of the inlet to poor near the cliffs. The circles and stars indicate computation points for the East/West and North/South survey lines, respectively. As the survey launch approaches the cliffs, the computation point spacing is shortened in order to increase the resolution of the results. The simulations could have been done for a single survey run at an arbitrary start time and speed, however, this may not have been a representative sample. Instead a 24-hour simulation was conducted at every computation point using a time interval of 60 seconds. At each computation point and for each epoch, the HDOP

and MHE were calculated. Thus the survey lines were analyzed for any start time during the day.

When the simulated survey launch reaches a cliff wall, 180° of the sky was blocked. Figure 4 shows the mask profile for the East/West survey line. The minimum mask angle is 10°, while the maximum mask angle of 90° occurs when the survey launch is at a cliff wall. The mask profile for the North/South line is essentially identical to that of the East/West profile, except for a 90° phase shift.

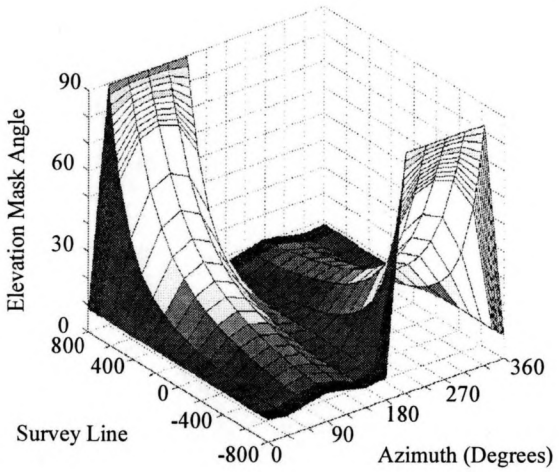

FIG. 4.- East/West Survey Line Mask Profile.

SIMULATION RESULTS

The simulation results have been grouped according to the survey line orientation, namely the East/West and the North / South survey line. If all of the data was presented, a three-axis (survey line position, time, and HDOP or MHE) figure would be required for each positioning mode. Instead of presenting the entire time series of HDOP and MHE values, the 95th percentile results are presented. Thus for each survey line position and positioning method the 95th percentile is plotted for the HDOP and MHE using contour graphs. The survey line position is plotted along the y-axis. Thus for the East/West line 800 m corresponds to the East cliff wall, and -800 m corresponds to the West cliff wall. The positioning methods are shown on the x-axis. The positioning methods are first grouped according to the satellites used (i.e., DGPS, DGPS + GLO, DGPS + DGEO, DGPS + DGLO, and DGPS + DGEO + DGLO). Then for each group of satellites the following four constraint options are used: N = none, H = height constraint, C = clock constraint, and H+C = height and clock constraint. The results left to right go from the least to the most augmented case.

East / West Survey Line

The availability (95% HDOP availability) results for the East/West survey line are shown in Figure 5. The results for DGPS alone are very good for horizontal distances greater than 300 m from the 300 m high cliffs. The 95% HDOP is normally less than 2, and once the height constraint is added it is normally less than 1. During the last 300 m of the survey line, the 95% HDOP reaches a value of 10. Even with height and clock constraints, the 95% HDOP remains above 2 towards the ends of the survey line.

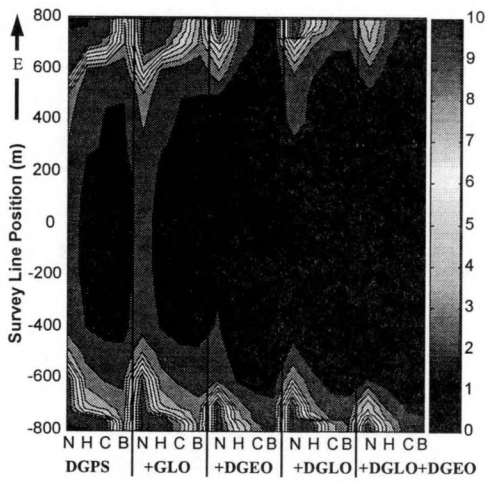

FIG. 5.- East/West Survey Line - 95% HDOP.

Augmenting DGPS with single point GLONASS does not improve the availability. This is due to the large difference between the DGPS and the single point GLONASS variances, 1 m^2 and 64 m^2 respectively. In the HDOP computation, the GLONASS satellites are de-weighted by 1/64 and thus do not improve the results. DGEO and DGLO both significantly improve the results, with DGEO slightly outperforming DGLO. From this result however, one cannot conclude that DGEO would always outperform DGLO. Although the additional satellite systems significantly improve the HDOP availability, constraints are still required to reduce the HDOP to reasonable levels near the cliffs. When the two constraints are intercompared, the clock constraint slightly outperforms the height constraint. This is expected due to the difference in the clock and height constraint variances of 1 m^2 and 4 m^2 respectively. In the most augmented case, namely DGPS + DGLO + DGEO + clock and height constraints, the 95% HDOP is better than 1 for the entire survey line. While HDOP is improved slightly in the middle of the inlet, the largest improvement is not as dramatic as near the cliffs. Thus the significant availability improvements are achieved during extreme masking conditions.

Figure 6 shows the 95% MHE for the East/West survey line. This figure shows that the reliability improvements achieved through augmentations occur over the entire survey line, not just close to the cliffs. With DGPS alone, the 95% MHE is greater than 90 m for the entire survey line, thus DGPS alone does not have the

high level of reliability required for many hydrographic survey missions. This is in stark contrast to the HDOP results, which showed that DGPS alone had a HDOP better than two for most of the survey line. This illustrates the danger in assessing only availability and ignoring the reliability of the positions. If reliability is ignored, quality assurance can drop below acceptable levels.

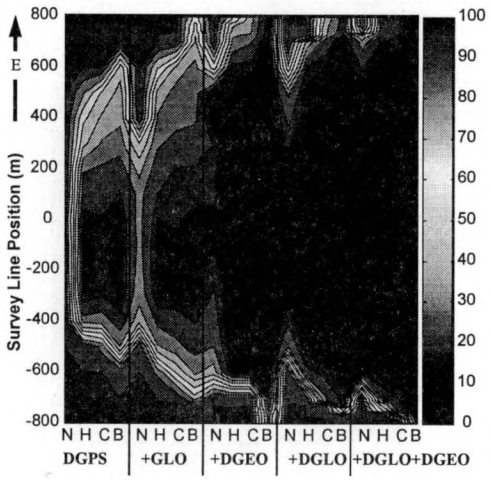

FIG. 6.- East/West Survey Line - 95% MHE.

Even when DGPS is augmented with both a height and a clock constraint, the 95% MHE still exceeds 100 m once the launch comes within 100 m of the cliff. Augmenting DGPS with single point GLONASS only marginally improves the results. Once DGPS is augmented with either DGEO or DGLO, the reliability improvement is remarkable. In order to obtain acceptable reliability numbers very close to the cliff, DGPS must be augmented with an additional satellite system and both constraints. As was the case for the availability analysis, the DGEO case again slightly outperforms the DGLO. When all three satellite systems and both constraints are used, the 95% MHE is below 10 m for the entire survey line, which is excellent. These results demonstrate the tremendous reliability improvements achievable by augmenting DGPS, both under benign and extreme masking conditions.

North / South Survey Line

The identical simulations were run for the North/ South survey line. The 95% HDOP and 95% MHE results are shown in Figures 7 and 8, respectively. The general availability and reliability results are the same as those of the East/West survey line. The only significant difference between the results of the two survey lines is the performance of the geostationary satellites. As was the case with the East/West survey line the DGEO results in the Northern direction are slightly better than DGLO. However, in the Southern direction, once the survey launch approaches the southern cliff, all the geostationary satellites are blocked, thus DGEO cannot improve the results in this case. This is an important result since, in the previous simulation, the DGEO augmentation was the best satellite

augmentation. This simulation highlights the major weakness of DGEO at the latitude tested, namely its relatively low elevation angle. This weakness becomes even more prominent at higher latitudes, since the geostationary satellites elevation angle is inversely proportional to latitude, as shown in Figure 2. In certain areas, such as the B.C. Coast, the majority of inlets run East/West and have steep southern shores.

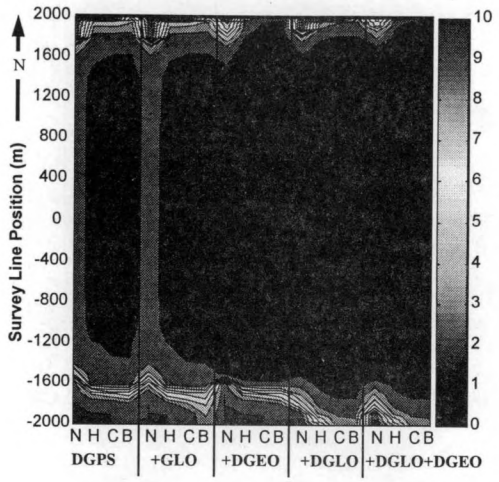

FIG. 7.- North/South Survey Line - 95% HDOP.

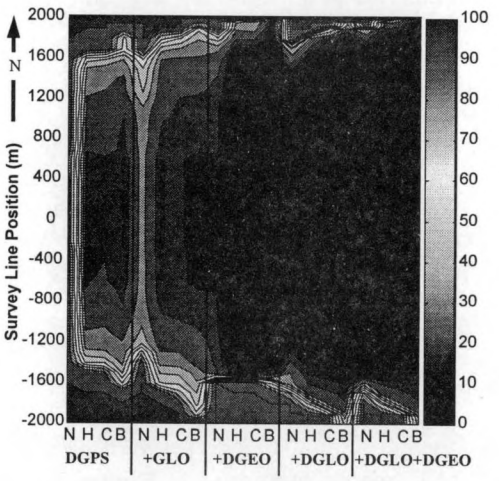

FIG. 8.- North/South Survey Line - 95% MHE.

These simulations have shown the theoretical improvements in availability and reliability that are achievable by augmenting DGPS with other satellite systems and constraints. In a previous paper where lower quality receivers were assumed as the basis for the simulation [RYAN et al 1997], single point GLONASS augmentation showed a significant improvement in both availability and

reliability. However, since high quality receivers were selected for the simulations described herein, single point GLONASS did not improve the results. While DGEO showed slightly better results than DGLO for the East/West simulations, its low elevation angle weakness was highlighted for the North/South simulation. Thus DGLO is the overall best satellite augmentation method for GPS at this time.

FIELD TEST DESCRIPTION

A field test was conducted to confirm the simulation conclusion that augmenting DGPS greatly improves both the availability and reliability of the positions. The test was conducted on July 25, 1997 in Saanich Inlet, B.C., with the assistance of the Canadian Hydrographic Service and the Canadian Coast Guard. The test consisted of a forty-minute trial using a survey launch from the Institute of Ocean Sciences (IOS) on Saanich Inlet on Vancouver Island. Typical sets of North/South and East/West survey lines were observed, as shown in Figure 9. The trajectory is tagged with various GPS time epochs to facilitate its analysis. Two Ashtech GG24™ integrated GPS/GLONASS receivers were used for the test. One was installed at the IOS as the reference station and the other was used on the survey launch. The distance between the two receivers was less than 15 km. The raw GPS and GLONASS code and carrier phase observables were processed using the University of Calgary's C^{3}NAVG^2™ software package (CANNON *et al.* 1997). The true trajectory was computed from the GPS carrier phase observables using the University of Calgary's FLYKIN™ software package. Due to the cliffs, GPS phase lock was often lost which precluded obtaining a fixed integer ambiguity solution. A float solution was used as the true trajectory instead, with a decimetre-level consistency between the forward and reverse solutions.

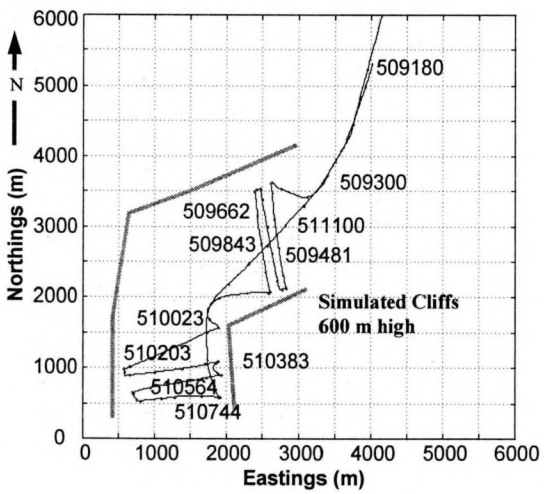

FIG. 9.- Field Test Trajectory.

Since augmenting GPS with single point GLONASS performed poorly during the simulations, this augmentation was not used for the field test. A clock

constraint was implemented by connecting rubidium frequency standards to the GG24™ receivers. A height constraint was implemented using tidal information. In total, the following eight methods were analyzed:

1) DGPS
2) DGPS + Height
3) DGPS + Clock
4) DGPS + Height + Clock
5) DGPS + DGLO
6) DGPS + DGLO + Height
7) DGPS + DGLO + Clock
8) DGPS + DGLO + Height + Clock

For each positioning method, the availability and reliability improvements were calculated. In addition to analyzing the data using the masking conditions provided by the actual terrain, 600 m high simulated cliffs were added to the trajectory and the data was reanalyzed for this case. The location of the simulated cliffs are shown in Figure 9. Thus two environments were analyzed, namely (i) the actual terrain and (ii) 600 m high simulated cliffs.

The availability improvement was determined by comparing the resulting HDOP for each positioning method. There are a number of ways to present the different HDOPs. Plotting the HDOP vs time for each positioning method shows all of the data, but doesn't capture the overall availability improvement. Quoting a single HDOP percentile shows the overall availability improvement, but only provide information on the cumulative distribution function. Thus to show the entire picture, cumulative probability distribution functions are used for each positioning method.

The reliability improvement is much harder to measure using real data. If a position is "reliable", it implies that there are no blunders in the observations. Thus to measure the reliability differences between the various methods, blunders were added to the observations. Each positioning method was processed separately and an attempt was made to detect the blunders and remove them from the position computation using epoch to epoch residual checking. The ramping blunder, shown in Figure10 was added to each GPS satellite, (PRN # 3, 17, 21, 23, 26, and 31), one at a time. In total, two ramping blunders were added to each GPS satellite, during the forty-minute test. The error was ramped up at a rate of 0.5 m/s until it reached a maximum of 50 m. It was then held constant at 50 m for 100 s and ramped back down to zero at a rate of -0.5 m/s. Each positioning method was processed using C^3NAVG^2™ six times, once for each GPS biased satellite. Since there were 600 s of biased data for each satellite and there were six satellites with blunders, there were 3600 s of biased data present for each positioning method. For each of these 3600 epochs, the horizontal position error (HPE) was calculated using the decimetre-level reference trajectory. The reliability improvement was determined by investigating the HPE cumulative distribution curves for each positioning method.

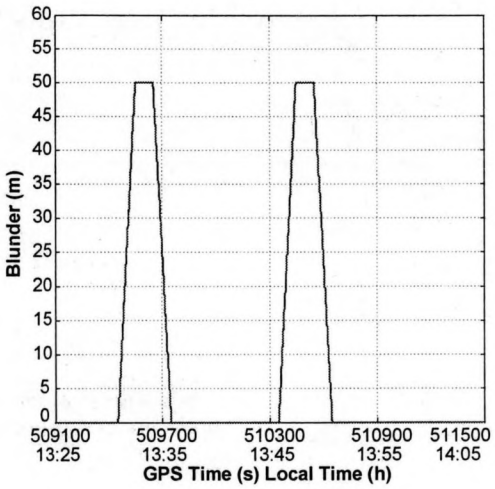

FIG. 10.- Blunder Added to GPS Satellites
(PRN # 3, 17, 21, 23, 26 and 31).

FIELD TEST RESULTS

Both the availability and reliability results are presented using cumulative distribution curves for the eight positioning methods and the two terrain profiles (actual and simulated cliffs). The DGPS methods are plotted using dashed lines and the DGPS + DGLO are plotted using solid lines. The four constraint methods use the following markers;

1) Star - no constraints
2) Circle - height constraint
3) X - clock constraint
4) Triangle - both height and clock constraints

Availability Results

When the actual terrain is analyzed, all the positioning methods tested have very good availability. The 95% HDOP for anyone of the methods is better than 2.7, as shown in Figure 11. At the lower HDOP values, there are differences between the various methods, with the combined DGPS + DGLO method out performing the DGPS method, as expected. The height and clock constraints produce similar results regardless of the constellations used. The addition of both constraints results in only marginal improvement compared with a single constraint. While augmenting DGPS with DGLO or constraints improves availability, it does not produce significant availability improvements for the actual terrain case.

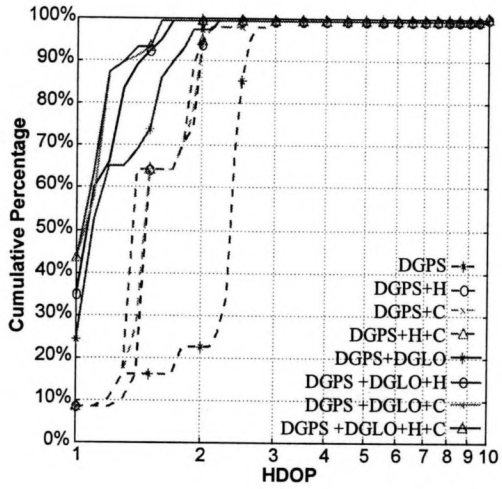

FIG. 11.- Actual Terrain - HDOP.

However, when the 600 m simulated cliffs are used, there is a much greater separation between the various methods, as shown in Figure 12. DGPS alone has a very low availability, the 95% HDOP value being greater than 10. Augmenting DGPS with a single augmentation, either DGLO or a constraint, improves the availability; in this case however, the 95% HDOP only improves to 3.5. Once DGLO and the constraints are combined, the 95% HDOP improves to 2.3. These results highlight an important fact, namely the real strength of augmentations in term of availability occur during extreme masking conditions.

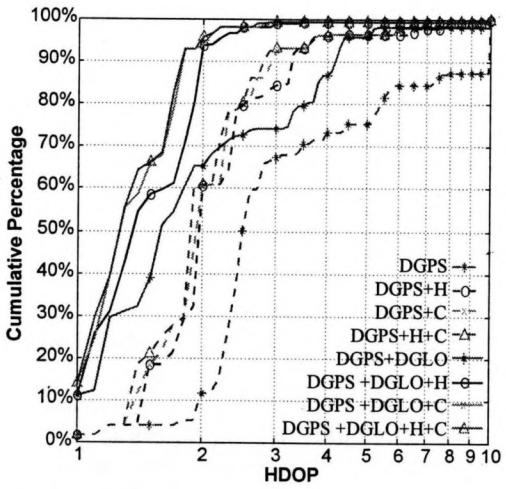

FIG. 12.- Simulated 600 m Cliffs - HDOP.

Reliability Results

The reliability improvements for the actual terrain and the simulated cliffs are presented in Figures 13 and 14, respectively. Unaided DGPS performs poorly in the actual terrain case; only 80% of the positions have a HPE less then 10 m. However, once a single augmentation is added, 95% of the positions have a HPE less than 1 m. While the DGLO method outperformed the unaided DGPS method, all of the augmentations performed very well. The blunders introduced were successfully detected.

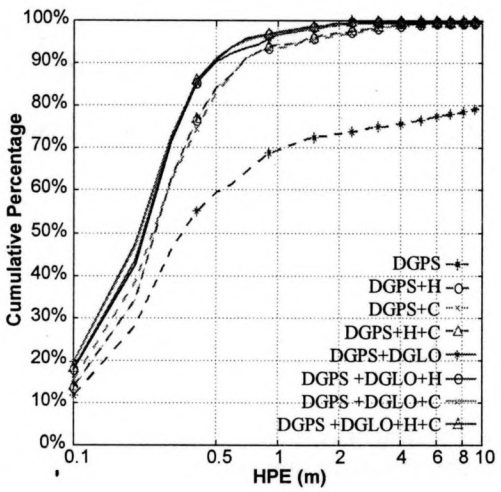

FIG. 13.- Actual Terrain -HPE
6 SVs During Ramps.

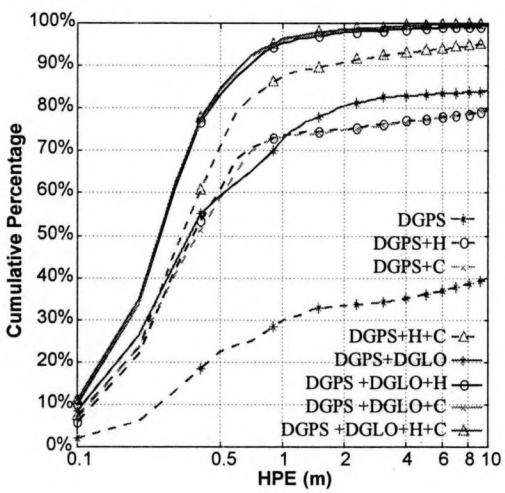

FIG.14.- Simulated 600 m Cliffs - HPE
6 SVs During Ramps.

As was the case with the availability analysis, the separation between the positioning methods increases once the simulated cliffs are added, as shown in Figure 14. In this case of unaided DGPS, only 40% of the positions have a HPE less than 10 m. When DGLO is added, the reliability of the positions is greatly improved, with 80% of the positions having a HPE less than 10 m. The 95% HPE improves to 1.0 m once DGLO and at least one constraint are added to DGPS. Even with the extreme masking conditions created by the simulated cliffs, reliable positions are still possible.

CONCLUSIONS

The use of the 15-satellite GLONASS constellation available during the simulations and field test to augment DGPS greatly improved both the reliability and the availability of positioning. While augmenting DGPS always improves the availability and reliability, the most significant improvements are achieved during poor masking conditions. From the results of both the simulations and field test, augmenting DGPS with DGLO and height and clock constraints fulfils the hydrographic horizontal accuracy requirements specified by the International Hydrographic Organization for all orders of survey, even under adverse masking conditions.

On-going work involves improving the reliability algorithm by utilizing a filter to improve blunder detection and exclusion by taking into account launch dynamics.

References

CANNON, M.E., G. LACHAPELLE and M. PETOVELLO (1997) Manual for C^{3}NAVG^{2TM} - Combination of Code and Carrier Phase Measurements for Navigation Using GPS and GLONASS. Department of Geomatics Engineering, the University of Calgary.

LEICK, A. (1995) GPS Satellite Surveying, 2nd Edition. John Wiley & Sons, Inc.

International Hydrographic Organization (1998). Special Publication 44 (S44), 4th edition, International Hydrographic Bureau, Monaco.

MORLEY, T. and G. LACHAPELLE (1997) GPS Augmentation with Pseudolites for Navigation in Constricted Waterways. Navigation, The Institute of Navigation, Alexandria, VA, 44, 3, 359-372.

RYAN, S., M. PETOVELLO and G. LACHAPELLE (1998) Augmentation of GPS for Ship Navigation in Constricted Waterways. Proceedings of National Technical Meeting, The Institute of Navigation (January 21-23, Long Beach, CA), 459-467.